Structural Stability Assessment of a Masonry Chimney Subjected to Shocks by Vibration Measurements

F. Telch[1], G. Lacidogna[1,*] and O. Rösch[2]

[1]Department of Structural, Geotechnical and Building Engineering, Politecnico di Torino, 10129 Torino, Italy

[2]Materials Testing and Research Institute, Karlsruhe Institute of Technology, 76131 Karlsruhe, Germany

Abstract: Nowadays buildings can be stressed and shocked in different ways. Rail and road traffic, demolition work, machines, bells, wind and human movement itself can burden structures and disturb people. Not only a vibration prognosis, but also a monitoring during certain work is important to ensure buildings' stability. A masonry chimney subject to shocks due to demolition works of surrounding halls was examined by using a new vibration measuring technique. This paper describes this new technique and its application during monitoring. For the measurement technique, the limit values of the German standard DIN 4150-3 were used and the events where this reference values exceeded, were examined in detail. A dynamic analysis of the structure, where the natural frequencies and their modal masses were determined, shows that the frequency-dependent reference values of the German standard DIN4150-3 for the protection of structures, include a relatively high safety factor. A possible exceeding of the values does not immediately lead to a loss of stability.

Keywords: Tall structures, Masonry chimney, Structural stability, Structural monitoring, Vibration measurements.

1. INTRODUCTION

The carrying capacity of civil engineering structures can be adversely affected by different factors. Not only static loads but also dynamic ones can be the causes [1]. The owners want their buildings always "healthy" or they want to protect a part of the building from shocks. That is why a structural health monitoring (SHM) is necessary nowadays. The SHM began to be extensively applied in the early 1990s after the technology evolved significantly. Software has also been developed in recent years that has made it easier to process the handling of data [2]. Initially, the monitoring was specifically designed for bridges including the famous cases of Rion-Antirion Bridge, Tamar Bridge, or Alamillo Cable-Stayed Bridge, among others [3-7], and constructions of particular importance, such as dams or other public buildings [8, 9].

Nowadays anyone can request a monitoring because their costs are low. On the basis of a monitoring it is possible to analyze the modal properties of a structure. The modal parameters and their derivatives depend on the health of the building. If their change over time, there is a sign that the structural conditions are changing, and they could be damaged. It may also be possible to localize and sometimes quantify the damage [10-15].

*Address correspondence to this author at the Department of Structural, Geotechnical and Building Engineering, Politecnico di Torino, 10129 Torino, Italy;
Tel: +39 011 090 4871;
E-mail: giuseppe.lacidogna@polito.it

As regards the building shocks modalities they vary depending on the type of source of exposure and dynamic characteristics of buildings themselves. In order to be able to carry out a correct monitoring, which is necessary for the prediction of crack formation, the following aspects have to be considered more closely:

Mechanism and propagation of excitation

- Shocks are the release of energy, which can spread in air, liquids and ground. In case of propagation in air, it appears as a load; on the other hand, in case of propagation in subsoil, a motion is transmitted to foundations. Therefore, the type of source influences the behaviour of different components.

Deterministic and aleatory nature of the phenomenon

- Deterministic vibrations are those determined by mathematical formulations, like harmonic and periodic vibrations, whereas aleatory vibrations are determined by probabilistic statistical parameters, for example stationary and non-stationary vibrations. In reality, the measured vibrations often consist of a superimposition of several of the above-mentioned modes of vibration [16].

Duration of the phenomenon

- Two fundamental effects of a shock are the achievement of resonance and materials fatigue.

E-ISSN: 2409-9821/18

Resonance is only achieved with long, continuous excitations. The minimum duration depends mostly on the first natural frequency f_0 of the buildings and on its degree of damping ς_0. If the duration of shocks is higher than $5\tau_0$, then this effect can be achieved. In this case, τ_0 is determined as follows:

$$\tau_0 = \frac{1}{2 \cdot \pi \cdot \varsigma_0 \cdot f_0} \quad (1)$$

- If the excitation duration does not exceed the constant of time τ_0 for five times, then one speaks of short-term shocks. However, several subsequent short-term shocks can cause problems with materials fatigue.

Spectral distribution of frequencies

- Each type of source is precisely defined in an amplitude spectrum over a specific range of frequencies. Thus, according to Italian standard UNI 9916: 2014, road and rail traffic can range between 1 and 300 Hz, driving in of piles between 1 and 100 Hz, and for demolition work where masses can fall between 1 and 20 Hz [17].

In this paper a masonry chimney during demolition work of surrounding halls has been examined by using a new vibration measuring technique. Therefore, the authors try to perform a new methodology expressly depicted for monitoring a tall masonry structure under shocks. But it is worth noting that to analyze the damage evolution on historical masonry structures there are other non-destructive methods, such as the Acoustic Emission (AE) technique. In the past one of the authors has produced several studies applying AEs as in situ monitoring system to develop a reliable evaluation of the state of conservation and damage of masonry structures and their evolution in time [18-22]. In addition, in the belief that more advanced results can be achieved by using different techniques, other studies have already been carried out to put together the monitoring of concrete structures by using AEs with experimental and numerical modal frequency variation analysis [14, 15].

A feasible idea is that in the future also AEs and shocks analysis techniques could be applied together to have a wider picture of the damage, considering both sudden and delayed effects due to shocks produced by environmental and anthropic actions.

Finally, the authors wish to say that deepening these monitoring techniques, and putting them in

Figure 1: Satellite image of the „Harsch-Steinzeugwerk“ with the chimney (yellow circle).

relation with appropriate methods of calculation, in the future it will be increasingly possible to predict and anticipate anomalous behavior of civil structures. This also in order to avoid and prevent disastrous phenomena such as those that have recently hit Italian infrastructures, see the disastrous collapse of the "Morandi Bridge" on the Polcevera river in Genoa on August 14, 2018.

2. DESCRIPTION OF THE ANALYZED BUILDING

In the German town of Bretten, about 23km northeast of the city of Karlsruhe in Baden-Württemberg lies the idle Harsch-Steinzeugwerk, which was built in 1926 (Figures **1**, **2**). In 2016, the owner decided to demolish the mighty Steinzeugwerk and redesign the area into a new residential and commercial space. On the 26.000 m^2 site, only the large masonry chimney remained to commemorate the glorious past of this company.

According to implementation plans [23], the 54-year-old masonry chimney protrudes 30 meters from the ground. Its diameter is 2.56 m at the bottom and 1.36 m at the top. The wall has four thickness jumps over its height. Between the jumps the thickness remains constant, it is equal to 50 cm at the bottom, and only 18 cm at the top. Table **1** shows the sections with the individual wall thicknesses.

Table 1: Geometric Characteristics of the Chimney

Section	High [m]	Segment length [m]	Thickness [m]
1	0 – 1	1	0.50
2	1 – 4	3	0.38
3	4 – 14	10	0.31
4	14 – 22	8	0.25
5	22 – 30	8	0.18

The base is conical and it is 3.55 m integrated into the ground. It is stored on a 0.8 m thick plate with a diameter of 4.8 m. In the base there is a 1.00 m wide and 2.25 m high supply air opening. In the lower area, a 12 cm thick and 2.30 m high, low-reinforced cuff was later attached to strengthen the tower in order to protect it.

Subsoil reports, statics and material investigations were not found. Therefore, there is no precise information on applied loads, stress resistance of the masonry, admissible ground stress and soil, or material stiffness.

The chimney was renovated in 1995 after cracks were formed due to storms. It is believed that the cuff described above was built after this event. From 1995, the chimney also served as a carrier of a mobile phone system, which has meanwhile been dismantled. For this reason, as reinforcement, approximately every 110

Figure 2: The chimney.

cm drawstrings were installed, which begin about 3.70 m above the cuff. Overall 23 drawstrings were used for the whole tower.

The chimney is currently no longer used and is therefore closed at the top by a concrete plug, except for a small opening for ventilation. The supply air opening is closed by soil and debris.

As previously described, there are several distinct cracks on the reinforced concrete cuff and at various locations above it. Striking is a pronounced vertical crack with a width of about 10 mm (Figure **3**). The cracks indicate that the ring tensile strength was exceeded at some point during the time. Evidently, the chimney also has an oblique position in the direction of the pronounced crack. Possibly, the above-mentioned mobile radio system, which was attached to this side, caused the formation of vertical cracks.

Figure 3: Cracks in the chimney.

3. DESCRIPTION OF THE DEMOLITION WORK

The chimney is surrounded by several buildings of the old stoneware factory. These were demolished with a demolition hammer. The destruction of components is taken place by means of transfer of impact energy of a sharp chisel. The excavators had a control device for adaptation of stroke rate and impact energy to the local conditions of use.

In addition, hydraulic demolition tongs were used, which are rotatable and perform the highest performance in every position. They break the material structure and separate it from the rest of the building because they can cut the reinforcement. They also shred different materials.

Both devices produce building masses that, in case of the old stone work, can fall down to a maximal height of about 5 m causing short-term vibrations. Their size can vary consistently: they can range from a few cubic centimetres to half a cubic meter [24, 25].

4. MEASURING DEVICE

Vibrations are completely described on the basis of amplitude, frequency and zero phase angle. Thus, vibration measurement technology deals with the measurement of paths, speeds, accelerations, forces, frequencies and phase angles [26]. Newer instruments convert these mechanical measurements into a proportional electrical quantity and then amplify and display the variables using electrical means.

The main advantages of an electrical measurement in contrast to a mechanical acting device are the following ones:

- Measuring device can be kept light and small;
- Measuring sensitivity is greater due to the use of electronic amplifiers;
- Multiple quantities, remote measurements and registrations can easily be performed [27].

A novelty of this study is the creation of a new measuring technique, which was specially produced for these kinds of problems.

In the case of the masonry chimney, a "SM6 Sensor Nederland" speed accelerometer sensor was used which can measure three directions simultaneously: two in the horizontal direction (H1 = v_x and H2 = v_y) and one in the vertical direction (V3 = v_z). The sensor was positioned on the cuff, at a height of 2.30 m, which can be seen in Figure **3**. This was connected to a measuring card of the "National Instrument" producer. Then, it was connected to a computer equipped with National Instrument's software DIAdem™. It is an

interactive software that allows one to measure, find, and manage data. This software also offers the possibility to analyse the data mathematically and graphically. It also consists of a script to automate repetitive applications with a partly proprietary programming language and partly VBScript language [28, 29].

For this monitoring, on "DIAdem DAC" interface, predefined circuit diagrams have been linked with data, system and control lines, so that the desired goal is achieved [30]. The aim was to store individual vibration events during continuous measurement in different files, and at the same time to emit an acoustic signal, to alert the worker that they have exceeded the allowable shock and need to check if any damage has occurred. In addition, the residents can be alarmed and possibly evacuated. An event includes measurements recorded one second before the limit is exceeded and five seconds after exceedance.

Among other things, the circuit diagrams define the sampling rate, thus the number of measurements per second. The sampling rate was set at 500 values per second. This results in 3000 values for six seconds of recording time. Incoming electrical quantities are transformed by means of a further circuit diagram into usable speed variables. These are then examined and, as soon as they exceed the limits reported in DIN 4150-3 [31], storage starts and the alarm is triggered. Therefore, as DIAdem DAC creates a file, all measured data are buffered, and as soon as the limit is exceeded, all data is deleted to one second before the reference value passed. After five seconds of the limit crossing, the measurement is stopped. A script was then used to write an infinite loop, with which one can restart the measurement over and over again and at the same time a new file is created. The names of these files include the time and date of application [32].

5. MONITORING PROCESS

Before the actual continuous measurement was started, the natural vibration of the chimney was measured with an accelerometer after a short calibration time of about 4 minutes. This was positioned on a steel bar, at a height of about 19 m, being part of a ladder which was installed on the structure. In Figure **4**, the measurement is shown [33].

The measured data come from time-discrete, finite signals, thus signals that are defined only at specific, equidistant times. The amplitude spectrum can usually be created with the discrete Fourier transform (DFT). The DFT processes a sequence of N numbers by representing them as values of a polynomial with complex coefficients. The polynomial can then be represented as a time-continuous periodic function and then transformed.

To speed the operation up, a Fast Fourier Transform (FFT) can be used. There are different methods of FFT that bear the name of their developers. In this case the FFT Hanning method was used [34].

The amplitude spectrum is shown in Figure **5**. From here one can see that the natural frequencies are approximately: 1.10 Hz, 4.55 Hz and 11.46 Hz.

In literature there are various references, such as [35, 36], which describe how to determine dynamic parameters from measurements using different vibration measurement techniques. Other books, such as [16] and [37] identify and describe these parameters in numeric way.

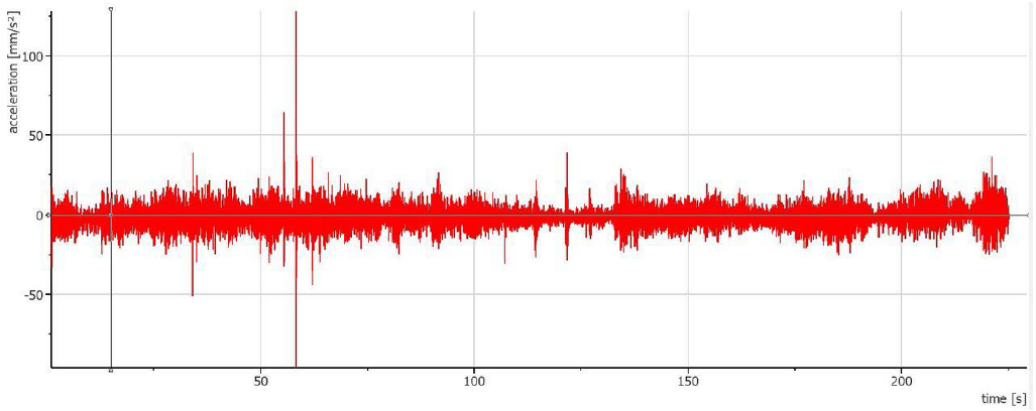

Figure 4: Vibration measurement for determining the natural frequency.

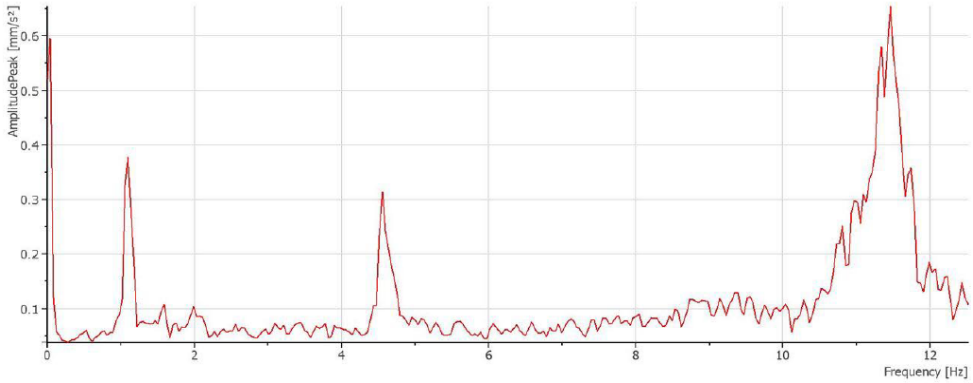

Figure 5: Amplitude spectrum of the vibration measurement.

If the first natural frequency is f_0 = 1.10 Hz and the degree of damping is set equal to ς_0 = 0.02, the constant of the time τ_0 can be derived from Eq. 1 as follows:

$$\tau_0 = \frac{1}{2 \cdot \pi \cdot \varsigma_0 \cdot f_0} = \frac{1}{2 \cdot \pi \cdot 0.02 \cdot 1.10} = 7\ sec \tag{2}$$

A falling mass causes a shock that works well under $5\tau_0 = 5 \times 7 = 35$ seconds; therefore, limits for short-term shocks, and not for permanent one, may be used [17].

The masonry chimney is a building with a special vibration sensitivity. According to the German standard DIN 4150-3 [31], the frequency-dependent limit oscillation speeds on foundations are the following ones:

- for $f_{vib} \leq 10Hz$

$$\rightarrow v_i \left[\frac{mm}{s}\right] = 3 \tag{3}$$

- for $10Hz < f_{vib} \leq 50Hz$

$$\rightarrow v_i \left[\frac{mm}{s}\right] = 0.125 \cdot \mathrm{f_{vib}} + 1.75 \tag{4}$$

- for $50Hz < f_{vib} \leq 100Hz$

$$\rightarrow v_i \left[\frac{mm}{s}\right] = 0.04 \cdot \mathrm{f_{vib}} + 6 \tag{5}$$

- for $f_{vib} > 100Hz$

$$\rightarrow v_i \left[\frac{mm}{s}\right] = 10 \tag{6}$$

These values were compared with the largest of the three measured vibration velocity components x, y, z [26].

The program described above cannot calculate the excitation frequency immediately and thus it cannot change the limits during monitoring. For safety reasons, it was decided to use the smallest reference value of 3 mm/s, because up to this vibration speed, no matter which excitation frequency is present, no problems should arise in any case. More accurate evaluation was carried out after monitoring. The demolition work with demolition hammer and tongs took about two and a half months. In this period, 34 events were recorded, so 34 times the vibration speed of 3 mm/s was exceeded.

6. EXPERIMENTAL RESULTS

As a first step, it was necessary to check whether these 34 events really overstepped the limit values as a function of the exciter frequency. However in most cases the limit has been exceeded only very slightly. To determine the excitation frequency, DIAdem performed a Fast Fourier transformation for the range between 0.5 sec and 1.5 sec.

If the amplitude spectra were created, one could determine the excitation frequency, that is the frequency with the highest amplitude. This value was then used to calculate the new limit through Eqs. (3-6).

In Figure **6**, for example, the event of June 7 at 11:57 am is shown. In this case, the oscillation speed is exceeded in horizontal direction H1. Considering the direction H1 with v_x = 3.304 mm/s and only the vibration itself (Figure **6**, top left and right sides), the decisive excitation frequency of 10.74 Hz is obtained. According to Eq. (4), the following oscillation speed can be determined:

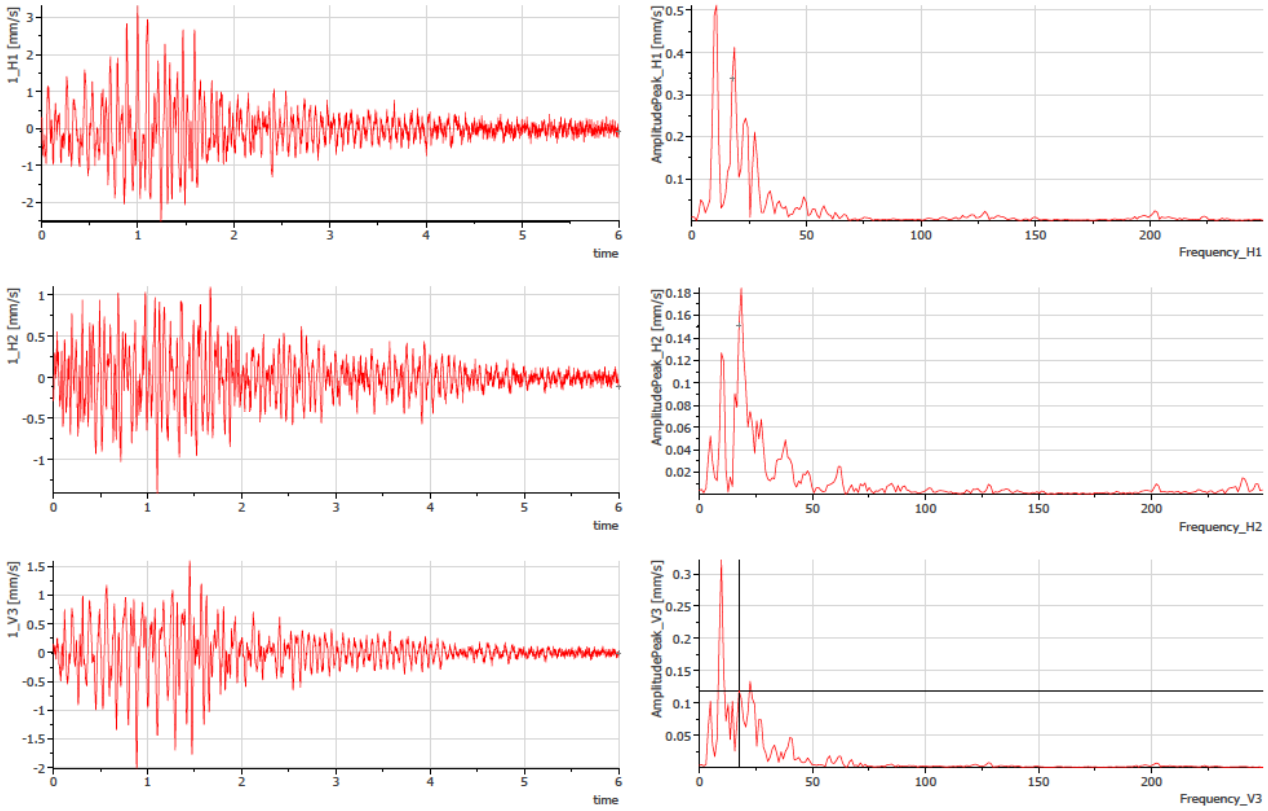

Figure 6: Event from June 7, 2017 at 11:57 am with the frequency spectrum on the right side.

$$v_{max,new} = 0.125 \cdot 10.74 + 1.75 = 3.093\, mm/s < 3.304\, mm/s \quad (7)$$

As can be seen, the existing oscillation speed is higher than the limit value, even if the difference is approximately 7% (= 0.211 mm/s). So further investigations must be carried out. This calculation method has been performed for all stored events and the results are listed in Table **2**.

In 23 cases, the vibration speed did not reach 4 mm/s. Among these, there were 4 events that surpassed the newly calculated value: these were on May 30 at 7:54 am, on June 6 at 12:57 pm, on June 7 at 11:57 am and on July 14 at 07:51 am. As can be seen in Table **2**, the oscillation speed of 3 mm/s in vertical direction is rarely overrun. Only on May 30 at 7:54 am, on June 8 at 8:58 am, and on June 13 at 08:29 am this case occurred. However, the calculated frequency of the third event brought a new limit of 3.2 mm/s, which makes it irrelevant. Mostly, vertical vibrations do not lead to problems because oscillation acceleration is added with the gravity acceleration. Otherwise, horizontal vibrations could be problematic. In five cases, there were a vibration speed over 5 mm/s. All of them were relevant: on June 6 at 10:30 am, on June 7 at 02:49 pm, on June 8 at 08:58 am and on July 18 at 08:02 am and at 08:03 am. Five events had a vibration speed between 4 and 5 mm/s, of which only one measurement was relevant: the event of June 2 at 09:40 am.

In summary: the alarm was triggered in 34 cases. Of these, only ten were relevant, since the frequency-dependent reference value was exceeded. All others can be classified as false alarms. In Figure **7** all results are shown graphically for better understanding. Basically, one can see a clear division into two large groups: the first one between 9 and 28 Hz and the second one between 230 and 250 Hz. It can be concluded that the excitement come from two different sources. The first group is due to falling masses. This is also supported by the shape of the vibration velocity diagrams, where clearly only one peak is present, as can be seen in Figure **6**. The second group may be the hydraulic breakers. As illustrated in Figure **8**, a plurality of consecutive peaks having a uniform temporal distance are clearly seen.

Table 2: Oscillation Speed that Triggered the Alarm and Calculation of the New Frequency-Dependent Reference Values

Event	Peak Speed	H1 [mm/s]	H2 [mm/s]	V3 [mm/s]	f [Hz]	$v_{max,new}$ [mm/s]	Exceeded
May 23, 09:37 am	H2	1.017	5.432	-0.233	195.313	10.000	No
May 23, 02:29 pm	H2	1.239	-3.389	-1.631	17.578	3.947	No
May 30, 07:54 am	V3	2.086	0.095	-3.579	11.719	3.215	**Yes**
May 30, 07:57 am	H2	0.985	3.579	0.074	147.461	10.000	No
June 02, 09:40 am	H1	-4.575	-4.246	-0.371	9.766	3.000	**Yes**
June 06, 10:30 am	H2	0.752	-5.549	1.673	15.625	3.703	**Yes**
June 06, 12:57 pm	H1	3.092	0.752	0.011	9.766	3.000	**Yes**
June 06, 02:30 pm	H2	1.112	3.420	1.303	26.367	5.046	No
June 07, 11:34 am	H1	3.357	-1.355	-2.245	24.414	4.802	No
June 07, 11:53 am	H1	-3.018	-0.053	1.472	26.367	5.046	No
June 07, 11:57 am	H1	3.304	-0.413	-0.752	10.742	3.093	**Yes**
June 07, 02:49 pm	H1	-5.951	2.404	-1.334	17.578	3.947	**Yes**
June 08, 08:58 am	H2	-4.501	8.620	-3.304	16.602	3.825	**Yes**
June 08, 10:33 am	H2	-2.213	4.204	-0.932	26.367	5.046	No
June 08, 11:26 am	H2	-1.991	4.088	0.720	249.023	10.000	No
June 08, 02:15 pm	H2	1.101	-4.024	-0.286	239.258	10.000	No
June 08, 02:33 pm	H2	-0.085	-3.537	-0.540	238.281	10.000	No
June 08, 03:03 pm	H2	-1.461	3.050	0.318	238.281	10.000	No
June 09, 09:05 am	H2	-1.048	3.240	-0.201	241.211	10.000	No
June 09, 09:08 am	H2	-0.529	-4.268	0.921	245.117	10.000	No
June 09, 09:13 am	H2	0.127	-3.791	-0.064	244.141	10.000	No
June 12, 09:49 am	H2	-1.101	3.071	0.572	248.047	10.000	No
June 12, 10:00 am	H2	-0.074	-3.050	-0.402	248.047	10.000	No
June 12, 10:28 am	H2	0.116	-3.293	-0.042	249.023	10.000	No
June 12, 10:32 am	H2	-0.180	-3.029	-0.339	242.188	10.000	No
June 12, 10:47 am	H2	0.868	-3.156	-0.191	242.188	10.000	No
June 12, 10:50 am	H2	-1.567	3.103	0.286	249.023	10.000	No
June 12, 10:55 am	H2	0.064	3.431	0.413	249.023	10.000	No
June 13, 08:29 am	V3	-0.265	1.535	3.018	11.719	3.215	No
June 13, 08:33 am	H1	-3.929	-1.059	-2.287	17.578	3.947	No
July 14, 07:51 am	H1	3.918	-1.779	2.203	9.766	3.000	**Yes**
July 17, 10:16 am	H1	-3.929	-0.127	-0.508	25.391	4.924	No
July 18, 08:02 am	H2	3.908	-6.671	-1.313	35.156	6.145	**Yes**
July 18, 08:03 am	H1	12.919	-8.588	0.275	222.656	10.000	**Yes**

In addition, it can be seen in Figure **7** that three points do not fall into these two cases: on May 30, at 07:57 am, May 23 at 09:37 am, and July 18 at 08:03 am, but it was not possible to detect the source which was the cause.

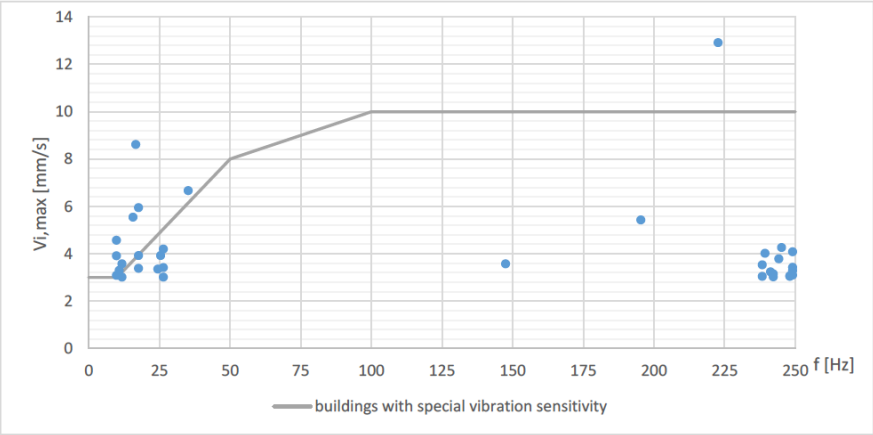

Figure 7: Graphic representation of the events.

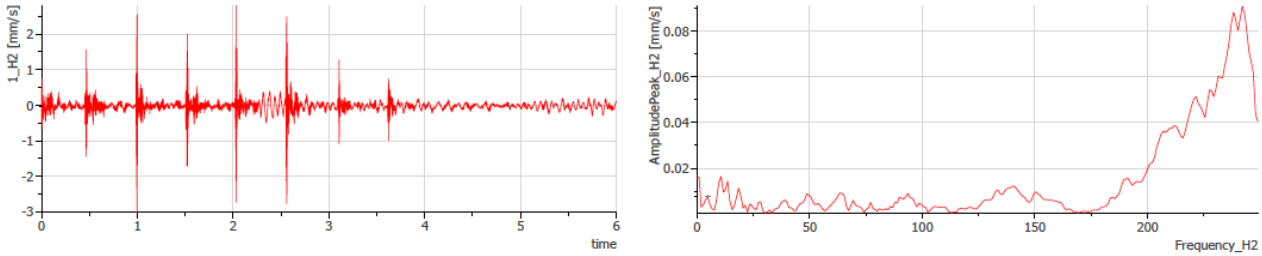

Figure 8: Horizontal vibration velocity of the event June 12, at 10:32 am.

7. NUMERICAL MODAL ANALYSIS

The ten events were examined more closely. For this purpose, they are converted as a static substitute load and applied to the building. First, the measured vibration velocities are transformed into acceleration with DIAdem. The acceleration response spectrum was determined using a Fast Fourier transform of the Hanning type. The natural frequencies and their associated modal mass were determined with a FE model by using the software LUSAS. The masonry chimney was modelled as a fixed cantilever from the subsoil. The finite elements "Thick Beam" were used. The diameter changes along the height. As an approximation, the tower is divided into several sections of constant diameter and 1m high. As a property of the finite elements, the elastic modulus and the density were given.

The stone strength was estimated with the Schmidt-Hammer. The Schmidt-Hammer is a rebound hammer, an instrument for non-destructive material testing, which measures the compressive strength point by point. It has been found that the bricks have a relatively high compressive strength of over 10 N/mm^2. The mortar is most likely a cement mortar with equally high strength. Thus, according to the German National Annex of the Eurocode 6, a standard masonry mortar III is obtained [38,39]. The chimney was built from solid bricks. In the case of one stone in the wall thickness direction, a characteristic compressive strength f_k of 6.0 N/mm^2 results from the table NA.D.3 of DIN EN 1996-3 / NA [39]. In the direction of the strength several stones were laid. Thus, this table value must be multiplied by 0.8 and one obtains a definite compressive strength of the wall of f_k = 6.0 × 0.8 = 4.8 N/mm^2. Based on the compressive strength, the modulus of elasticity was determined according to the German National Annex DIN EN 1996-1-1/NA: E = 4.8 × 1100 = 5280 N/mm^2 [38,39]. Finally, using a density of ρ = 1800 kg/m^3, the first four natural frequencies listed in Table **3** with the associated modal masses can be obtained. The modal shapes and frequencies are represented in Figure **9**.

Table 3: Natural Frequencies and Associated Modal Masses of the Chimney

Mode Number	Natural Frequency [Hz]	Modal mass M_m [%]
1	1.13	44.1
2	4.60	20.9
3	10.85	10.0
4	19.40	6.1

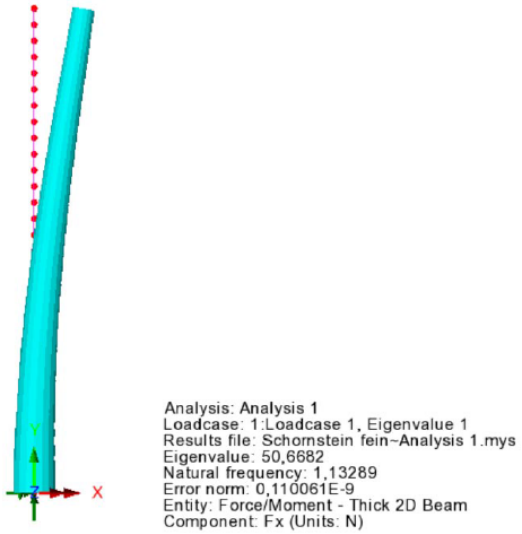

(a): First natural frequency

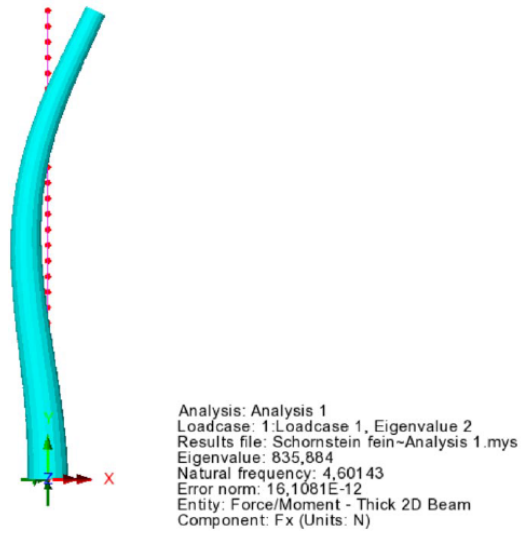

(b): Second natural frequency

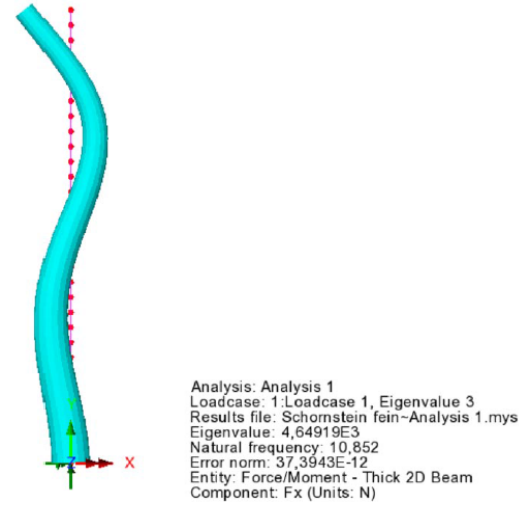

(c): Third natural frequency

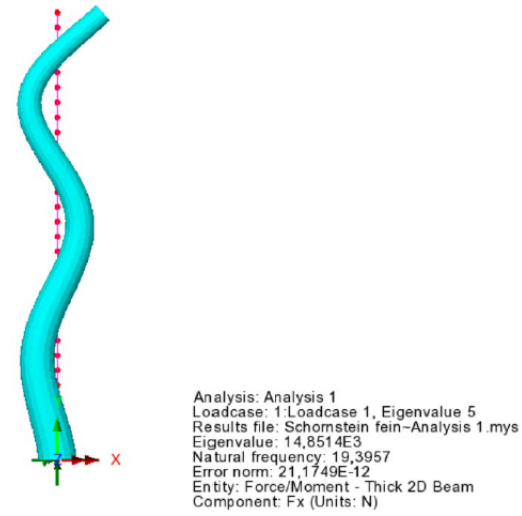

(d): Fourth natural frequency

Figure 9: Modal shapes and frequencies of the masonry chimney

As can be seen in Table **3**, the calculated natural frequencies almost coincide with the measured ones, so that one can guess that the assumed material properties are correct. The total mass of the chimney for the given geometry is 81.388 kg.

Due to existing geometry, not only compressive stresses but also circumferential tensile stresses occur, which should not exceed the permissible tensile strength. The fracture plane is perpendicular to the horizontal joints. However, as previously described and illustrated in Figure **3**, at the base, thus at the reinforced concrete cuff and at the masonry wall, cracks of several millimetres were found. These must be taken into account in the investigations, which means, tensile strength of the masonry is neglected.

The reinforced concrete cuff is cracked. Thus, only the reinforcement can absorb the tensile forces in the circumferential direction. According to implementation plan [23], and as shown in Figure **10**, a welded steel mesh ø6/15x15 cm, with a_s = 1.88 cm^2/m, was installed in the 12 cm thick cuff by bending it in a U-shape. This results in two layers with reinforcement. At the foot 2ø16 (A_s = 4.02 cm^2) were collocated. A reinforcing steel Bst500S with a characteristic yield strength of f_{yk} = 500 MPa was used. Considering a safety factor equal to 1.15, the yield strength to be used is f_{yd} = 435 MPa. Because the existing reinforcement cross-sectional area is A_s = 778 mm^2, it can absorb a tensile force of 338 kN.

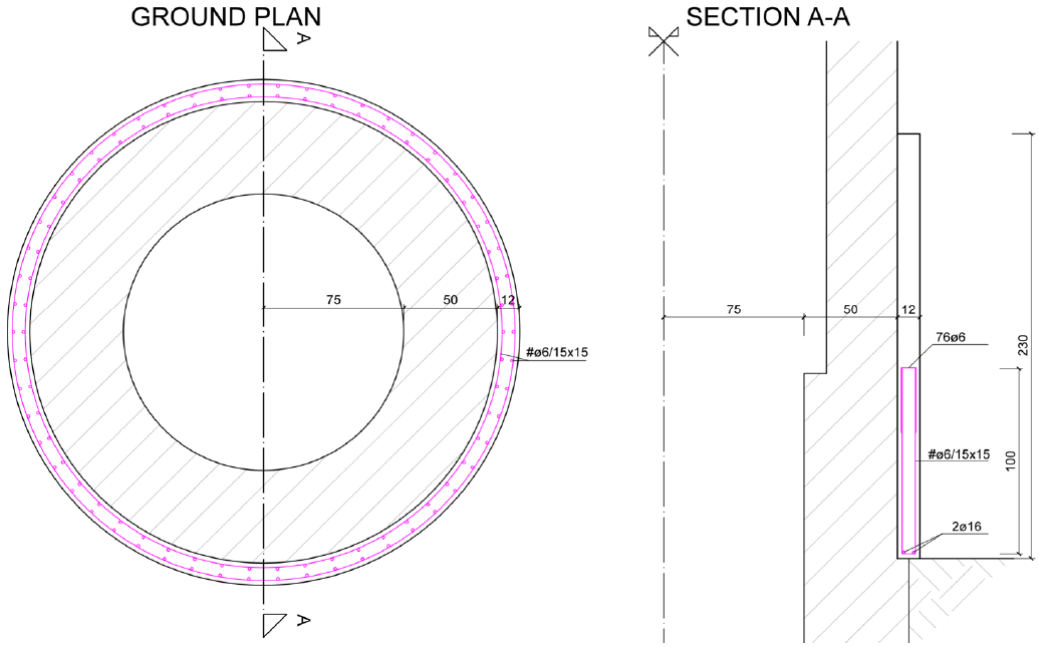

Figure 10: Detail of the concrete cuff.

Based on the previously calculated natural frequencies, the associated modal masses, the total mass M_{tot} and the amplitude spectra of acceleration, the static load F_i was determined for each natural frequency. The existing vibration can be seen as a seismic action. According to the German Eurocode [40] a damping measure of q = 2 can be used for masonry structures. This results in the following relation for the static load:

$$F_i = a \cdot \frac{M_m}{q} \cdot M_{tot} \tag{8}$$

Each force was applied on the top of the chimney. To calculate the compressive stresses and the tensile forces a new FE-model was defined. In this case the software RFEM of Dlubal Software were used to create the 3D model with the geometric characteristics written in Table **1**. This resulted in 4 values for each event, one per natural frequency. The final pressure at the foot of the chimney was determined using the Square Root Sum of Squares (SRSS) method:

$$\sigma = \sqrt{\sigma_1^2 + \sigma_2^2 + \sigma_3^2 + \sigma_4^2} \tag{9}$$

As an example the event of June, 07 at 11:57 am is considered. Table **4** shows accelerations according to the amplitude spectrum for each natural frequency. For each individual acceleration, the static force was determined by (8) and through the FE model the compressive stresses and tensile forces were found.

In Figure **11**, the 3D model is represented. It shows the compressive stresses due to the third natural frequency and the vibration of June, 07 at 11:57 am. Attention is drawn to the fact that the force in the model was entered as a line load, therefore the forces F were divided by the diameter of the chimney head. No single concentrated force was applied, as this does not give a truthful deformation, especially around the applied force zone. From the diagram of Figure **11**, the stress was obtained. This operation was used for the other three modes of oscillation, and using Eq. (9) the effective compressive stress due to vibration was determined.

Table 4: Compressive Stresses and Tensile Forces from June, 07 at 11:57 am

T [s]	a [m/s^2]	M_m [-]	F [kN]	σ [kN/m^2]	N_t [kN]
1.13	0.01	0.441	0.23	-4	0.3
4.60	0.94	0.209	8.00	-146	11
10.85	27.71	0.100	112.76	-2053	148
19.40	24.26	0.061	60.21	-1096	79

By using Eq. (9), a compressive stress of 2.3 MPa, and a tensile force of 168 kN, at the chimney base are obtained, which respectively are lower than the

masonry strength (4.8 MPa), and the steel plastic axial force (338 kN).

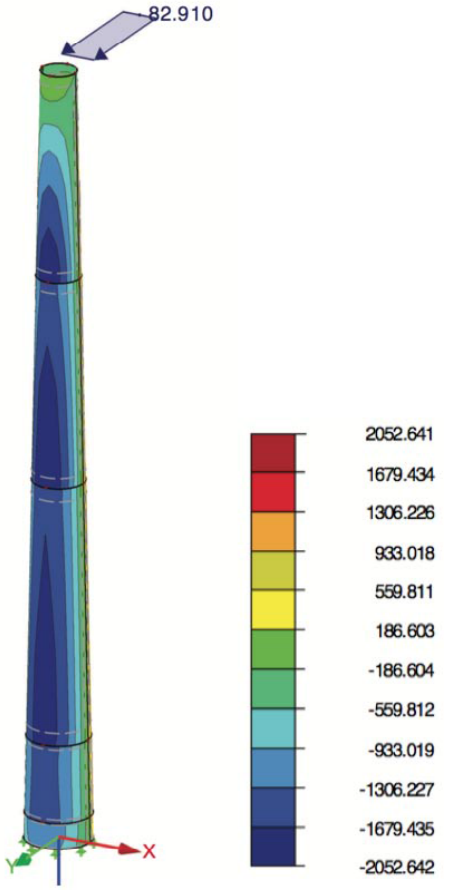

Figure 11: 3D – Model with the compressive stresses induced due the third natural frequency of the vibration on June, 07 at 11:57 am.

As can be seen, the existing loads do not exceed the associated admissible values, and thus it is proved that this event did not harm to the chimney.

In Figures **12** and **13**, the compressive stress and the tensile forces are shown. As can be seen, the permissible compressive stress of 4.8 MPa and the existing permissible tensile force of 338 kN were never reached. The most stressful event occurred on June 07, at 02:49 pm. In this case the oscillation speed reached in the horizontal direction H1 5.951 mm/s. Removing this event, one might assume that there is a relation between the oscillation speed and strength but instead are only the spectral accelerations factors that affect stress. The connection would be the lower the vibration velocity, the higher the loads.

CONCLUSIONS

Demolition work is one of many sources of vibration that can burden buildings and disturb people. Among other standards, the German standard DIN 4150/3 can be used for this assessment. This indicates frequency-dependent reference values of the vibration velocity. If these are exceeded, then damage to buildings may occur. However, these values are based on measurements made in the past, which results in them having a high safety factor to take into account that different variables, such as the mechanical properties of the subsurface, and the structural behaviour. For monitoring the masonry chimney, a specially developed algorithm was used, where individual events are stored in different files as soon as limit values are exceeded.

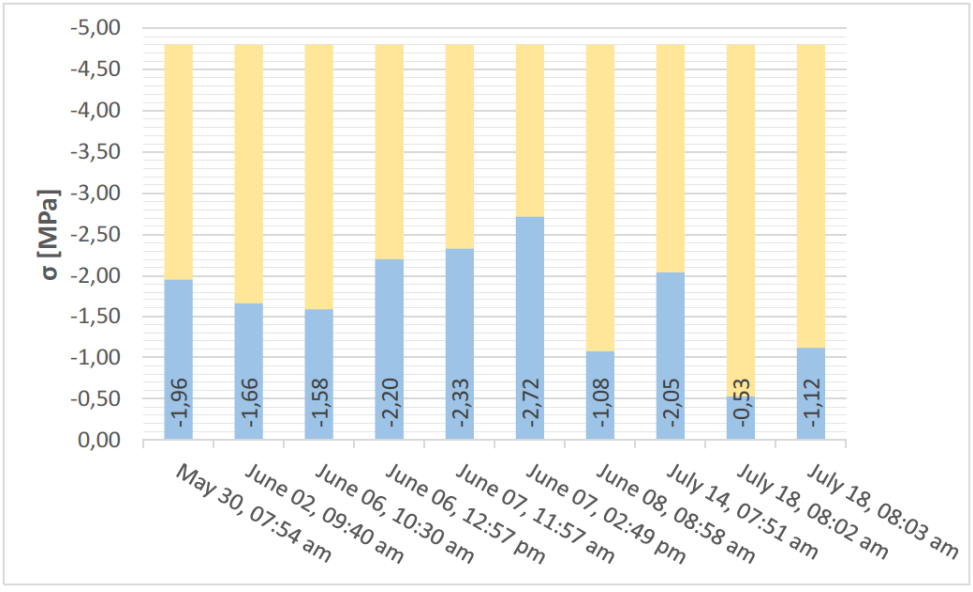

Figure 12: Existing compressive stress (blue), missing compressive stress to reach the permissible one (yellow).

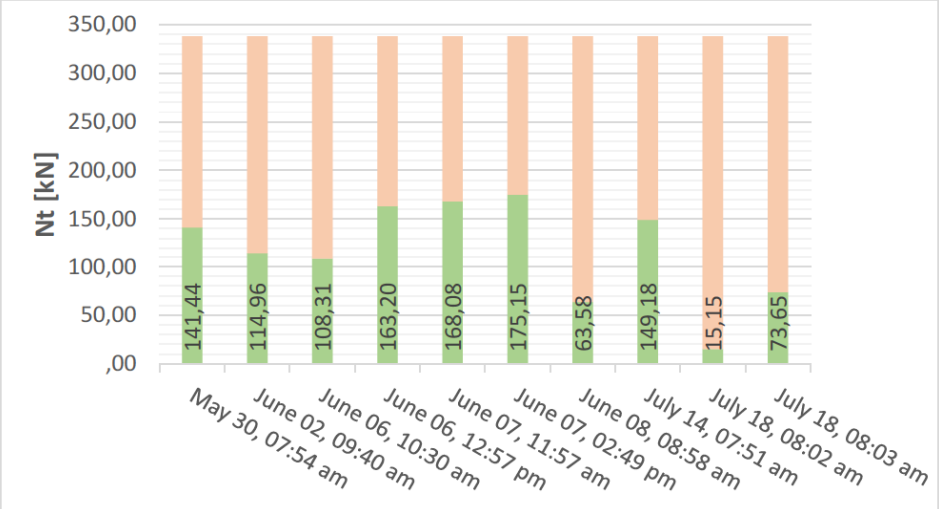

Figure 13: Existing tensile force (green), missing tensile force to reach the permissible one (grey).

This can also be used for other monitoring in the future. In about three months working, 34 events were saved. Among these, ten exceeded the frequency-dependent reference values.

These ten events were then examined more closely by calculating the compressive stresses and the tensile stresses in the circumferential direction. The calculations constitute a method to have more accurate information about stresses and forces. All the obtained results show that they do not exceed the permissible compressive stress, and the maximum tensile force that can be absorbed even if the speed was initially higher than the reference value. This was then confirmed by a local inspection. No new cracks were found here and the existing ones did not get larger. Thus it is proved that exceeding the reference values of the DIN 4150-3 does not immediately lead to a serious loss of stability.

ACKNOWLEDGEMENTS

This manuscript was synthesized from a Master Thesis, written in 2017 at Politecnico di Torino and at the Materials Testing and Research Institute (MPA Karlsruhe) of Karlsruhe Institute of Technology (KIT). Author of the thesis was Eng. F. Telch, while the supervisors were Prof. G. Lacidogna and Prof. O. Rösch [30].

REFERENCES

[1] Adams RD, Cawley P, Pye CJ, Stone BJ, A vibration technique for non-destructively assessing the integrity of structures. Journal of Mechanical Engineering Science, 1978; 20: 93-100. https://doi.org/10.1243/JMES_JOUR_1978_020_016_02

[2] Andersen JE, Fustinoni M, Structural Health Monitoring Systems. COWI-Futurec, L&S S.r.l. Servizi Grafici, Milano, Italy, 2006.

[3] Le Diourion T., The health monitoring of Rion-Antirion Bridge. Proc. 23rd Conference and Exposition on Structural Dynamics (IMAC - XXIII), Orlando, Florida, 2005.

[4] Brownjohn JMW, Carden P, Real-time operation modal analysis of Tamar Bridge. Proc. 26th Conference and Exposition on Structural Dynamics (IMAC - XXVI), Orlando, Florida, 2008.

[5] Cross EJ, Koo K, Brownjohn JMW, Worden K, (2010). Long-term monitoring and data analysis of the Tamar Bridge. Mechanical Systems and Signal Processing, 2013; 35: 16-34.

[6] Casas JR, Aparicio AC, Monitoring of the Alamillo cable-stayed bridge during construction. Experimental Mechanics, 1998, 38: 24-28. https://doi.org/10.1007/BF02321263

[7] Casas JR, Aparicio AC, Rain-wind induced vibrations in the Alamillo cable-stayed bridge (Sevilla, Spain). Assessment and remedial action. Structure and Infrastructure Engineering, 2010; 6: 549-556. https://doi.org/10.1080/15732470903068607

[8] CIGB ICOLD, Dam monitoring. General considerations. International Commission on Large Dams, Bulletin 60, Paris, 1988.

[9] Brownjohn JMW, Carden EP, Goddard RC, Oudin C, Real-time performance monitoring of tuned mass damper system for a 183m reinforced concrete chimney. Wind Engineering and Industrial Aerodynamics, 2010; 98: 169-179. https://doi.org/10.1016/j.jweia.2009.10.013

[10] Cawley P, Adams RD. The location of defects in structures from measurements of natural frequencies. Journal of Strain Analysis, 1979; 14: 49-57. https://doi.org/10.1243/03093247V142049

[11] Lilley DM, Adams RD, Larnach WJ. Location of defects within embedded model piles using a resonant vibration technique. Proc. 10th World Conference on Nondestructive Testing, Moscow, Russia, 1982.

[12] De Roeck G, The state of the art of damage detection by vibration monitoring: the SIMCES experience. Structural Control and Health Monitoring, 2003; 10: 127-134. https://doi.org/10.1002/stc.20

[13] Catbas FN, Kijewski-Correa T, Aktan AE. Structural Identification (ST-Id) of Constructed Facilities. Approaches,

Methods and Technologies for Effective Practice of St-Id. ASCE SEI Committee on Structural Identification of Constructed Systems, 2011.

[14] Lacidogna G, Piana G, Carpinteri A. Acoustic emission and modal frequency variation in concrete specimens under four-point bending. Applied Sciences-Basel, 2017; 7: 339. https://doi.org/10.3390/app7040339

[15] Lacidogna G, Piana G, Carpinteri A. Damage monitoring of three-point bending concrete specimens by acoustic emission and resonant frequency analysis. Engineering Fracture Mechanics, 2018. https://doi.org/10.1016/j.engfracmech.2018.06.034

[16] Kramer H, Angewandte Baudynamik, Grundlagen und Praxisbeispiele, Edition 2, Wilhelm Ernst & Sohn, Berlin, 2013. https://doi.org/10.1002/9783433602690

[17] UNI 9916 Rules, Criteri di misura e valutazione degli effetti delle vibrazioni sugli edifici, 2004 (in Italian)

[18] Carpinteri A, Lacidogna G. Structural monitoring and integrity assessment of medieval towers. Journal of Structural Engineering (ASCE), 2006; 132: 1681-1690. https://doi.org/10.1061/(ASCE)0733-9445(2006)132:11(1681)

[19] Carpinteri A, Lacidogna G. Damage evaluation of three masonry towers by acoustic emission. Engineering Structures, 2007, 29: 1569-1579. https://doi.org/10.1016/j.engstruct.2006.08.008

[20] Carpinteri A, Grazzini A, Lacidogna G, Manuello A. Durability evaluation of reinforced masonry by fatigue tests and acoustic emission technique. Structural Control and Health Monitoring, 2014; 21, 950-961. https://doi.org/10.1002/stc.1623

[21] Han Q, Xu xJ, Carpinteri A, Lacidogna G. Localization of acoustic emission sources in structural health monitoring of masonry bridge. Structural Control and Health Monitoring, 2015; 22: 314-329. https://doi.org/10.1002/stc.1675

[22] Carpinteri A, Lacidogna G, Manuello A, Niccolini G. A study on the structural stability of the Asinelli Tower in Bologna. Structural Control and Health Monitoring, 2016; 23: 659-667. https://doi.org/10.1002/stc.1804

[23] Implementation plans from 1962, draw by Ooms Ittner & Cio, Köln.

[24] Schröder M, Pocha A, Deutscher Abbruchverband e. V., Abbrucharbeiten, Grundlagen, Planung, Durchführung, Ed. 3, Verlaggesellschaft Rudolf Müller GmbH & Co. KG., Köln, 2015.

[25] Korth D, Lippok J. Abbrucharbeiten, Vorbereitung und Durchführung, Ed. 2, VEB Verlag für Bauwesen, Berlin, 1987.

[26] Kuttner T, Praxiswissen Schwingungsmesstechnik, Fakultät für Maschinenbau Universität der Bundeswehr München, Springer Vieweg, Neubiberg, 2015. https://doi.org/10.1007/978-3-658-04638-5

[27] Hübner E. Technische Schwingungslehre in ihren Grundzügen, Springer Verlag, Berlin/Göttingen/Heidelberg, 1957. https://doi.org/10.1007/978-3-642-92703-4

[28] National Instruments, NI DIAdem, Erste Schritte mit DIAdem, National Instruments Corporation, München, 2014.

[29] National Instruments, NI DIAdem, Daten finden, analysieren und dokumentieren, National Instruments Corporation, München, 2014.

[30] National Instruments, NI DIAdem, Daten erfassen und visualisieren, National Instruments Corporation, München, 2014.

[31] DIN 4150-3 rules, Vibrations in buildings – Part 3: Effects on structures, 2016 (in German).

[32] Telch F. Vibration measurements and their assessment concerning the effect on a masonry chimney, Masterthesis, Department of Structural, Geotechnical and Building Engineering (DISEG), Politecnico di Torino, and Materials Testing and Research Institute (MPA), Karlsruher Institute of Technology, Tutors: Lacidogna G. (DISEG) and Rösch O. (MPA).

[33] Rösch O. Prüfbericht: Schwingungsmessung und Erschütterungsüberwachung an einem bestehenden Ziegelschornstein im Zuge der Rückbaumaßnahmen am Steinzeugpark in Bretten, Karlsruhe, 2017.

[34] Das A. Signal Conditioning. An Introduction to Continuous Wave, Communication and Signal Processing, Springer Verlag, Berlin - Heidelberg, 2012.

[35] Haupt W, Bodendynamik, Grundlagen und Anwendung, Friedr. Vieweg & Sohn, Braunschweig/Wiesbaden, 1986.

[36] Korenev BG, Rabinovic IM, Baudynamik, Handbuch, VEB Verlag für Bauwesen, Berlin, 1980.

[37] Stempniewski L., Haag B., Baudynamik-Praxis, Mit zahlreichen Anwendungsbeispielen, Bauwerk Verlag GmbH, Berlin, 2010.

[38] DIN EN 1996-1-1/NA, National Annex –Nationally determined parameters – Eurocode 6: Design of masonry structures –Part 1-1: General rules for reinforced and unreinforced masonry structures. 2012.

[39] DIN EN 1996-3/NA, National Annex –Nationally determined parameters –Eurocode 6: Design of masonry structures – Part 3: Simplified calculation methods for unreinforced masonry structures. 2012.

[40] DIN EN 1998-1, Eurocode 8: Design of structures for earthquake resistance – Part 1: General rules, seismic actions and rules for buildings; German version EN 1998-1: 2004 + AC:2009.

Received on 11-11-2018 Accepted on 30-12-2018 Published on 31-12-2018

DOI: http://dx.doi.org/10.15377/2409-9821.2018.05.4